

Acyclic Bis(N₂O₂ chelate) Ligand for Trinuclear d-Block Homo- and Heterometal Complexes

Shigehisa Akine, Takanori Taniguchi, and Tatsuya Nabeshima*

Graduate School of Pure and Applied Sciences, University of Tsukuba, Tsukuba, Ibaraki 305-8571, Japan

Received November 16, 2007

We have synthesized a new type of acyclic bis(N₂O₂ chelate) ligand that affords a C-shaped O₆ site by the metalation of the N₂O₂ salamo sites. UV–vis titration clearly showed that complexation of H₄L with M^{II} (Mn^{II}, Co^{II}, and Ni^{II}) affords the 1:3 complex [LM₃]²⁺ in a cooperative fashion, whereas complexation with copper(II) gave two or more complexes in a stepwise fashion. The manganese(II) complex [LMn₃(OAc)₂(MeOH)₂] crystallizes in the triclinic system, space group *P* $\bar{1}$, with unit cell parameters *a* = 9.584(6) Å, *b* = 13.666(9) Å, *c* = 15.566(10) Å, α = 108.702(8)°, β = 95.255(4)°, γ = 101.023(8)°, and *Z* = 2, and the cobalt(II) complex [LCo₃(OAc)₂(EtOH)₂] · 2CHCl₃ crystallizes in the triclinic system, space group *P* $\bar{1}$, with unit cell parameters *a* = 13.291(6) Å, *b* = 13.913(7) Å, *c* = 14.599(8) Å, α = 88.27(2)°, β = 67.391(15)°, γ = 73.90(2)°, and *Z* = 2. In the crystal structures, three metal ions occupied both the N₂O₂ and O₆ sites of the ligand L⁴⁻. The resultant trinuclear complexes have a C- or S-shaped structure depending on the metal employed. The different nature of the N₂O₂ and O₆ sites of the ligand H₄L leads to the site-selective introduction of two different d-block transition metals. An X-ray crystallographic analysis revealed the structures of the two heterotrimeric complexes, [LZn₂Mn(OAc)₂(MeOH)₂] and [LCu₂Zn(OAc)₂(H₂O)].

Introduction

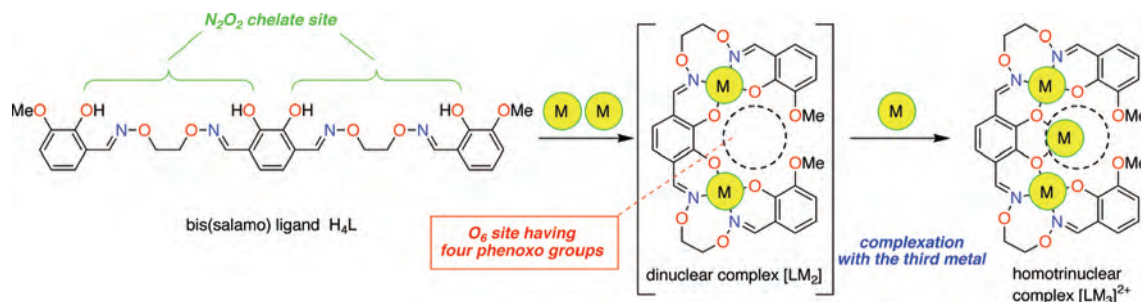
Salen-type N₂O₂ ligands coordinate to various kinds of transition-metal ions in a tetradentate fashion to produce stable complexes.¹ Some of these complexes serve as the catalysts of organic reactions,² models of the catalytic centers of metalloenzymes,³ nonlinear optical materials,⁴ and metallocenes.⁵ In recent years, salen complexes are also used as a building block of supramolecular structures⁶ or sensing of chiral organic molecules.⁷ A molecule containing two or more salen complex moieties is also fascinating because novel functions originating from the cooperation of several

metal centers are expected. In addition to an enormous number of bimetallic complexes of compartmental ligands,⁸ larger macrocyclic bis(salen),^{9–11} tris(salen),¹² and acyclic bis(salen)¹³ derivatives have been reported. Electrochemical studies clearly showed an interaction between the metal centers.⁹ The cooperative action of the metal centers in some of the salen oligomers was successfully utilized for the catalytic organic reactions.^{11,13,14}

* To whom correspondence should be addressed. E-mail: nabesima@chem.tsukuba.ac.jp.

- (1) (a) Pfeiffer, P.; Breith, E.; Lübke, E.; Tsumaki, T. *Liebigs Ann. Chem.* **1933**, 503, 84–130. (b) Pfeiffer, P.; Hesse, T.; Pfitzner, H.; Scholl, W.; Thielert, H. *J. Prakt. Chem.* **1937**, 149, 217–296.
- (2) For reviews of salen complex catalysts, see: (a) Jacobsen, E. N. *Catalytic Asymmetric Synthesis*; Ojima, I., Ed.; VCH: New York, 1993. (b) Katsuki, T. *Coord. Chem. Rev.* **1995**, 140, 189–214. (c) Jacobsen, E. N. *Acc. Chem. Res.* **2000**, 33, 421–431.
- (3) (a) Tsou, T.-T.; Loots, M.; Halpern, J. *J. Am. Chem. Soc.* **1982**, 104, 623–624. (b) Summers, M. F.; Marzilli, L. G.; Bresciani-Pahor, N.; Randaccio, L. *J. Am. Chem. Soc.* **1984**, 106, 4478–4485.
- (4) (a) Di Bella, S.; Fragalà, I. *Synth. Met.* **2000**, 115, 191–196. (b) Lacroix, P. G. *Eur. J. Inorg. Chem.* **2001**, 339–348.
- (5) Hoshino, N. *Coord. Chem. Rev.* **1998**, 174, 77–108.

- (6) (a) Morris, G. A.; Nguyen, S. T.; Hupp, J. T. *J. Mol. Catal. A* **2001**, 174, 15–20. (b) Splan, K. E.; Massari, A. M.; Morris, G. A.; Sun, S.-S.; Reina, E.; Nguyen, S. T.; Hupp, J. T. *Eur. J. Inorg. Chem.* **2003**, 2348–2351. (c) Sun, S.-S.; Stern, C. L.; Nguyen, S. T.; Hupp, J. T. *J. Am. Chem. Soc.* **2004**, 126, 6314–6326. (d) Cho, S.-H.; Gadzikwa, T.; Afshari, M.; Nguyen, S. T.; Hupp, J. T. *Eur. J. Inorg. Chem.* **2007**, 4863–4867. (e) Gianneschi, N. C.; Bertin, P. A.; Nguyen, S. T.; Mirkin, C. A.; Zakharov, L. N.; Rheingold, A. L. *J. Am. Chem. Soc.* **2003**, 125, 10508–10509. (f) Gianneschi, N. C.; Cho, S.-H.; Nguyen, S. T.; Mirkin, C. A. *Angew. Chem., Int. Ed.* **2004**, 43, 5503–5507. (g) Gianneschi, N. C.; Nguyen, S. T.; Mirkin, C. A. *J. Am. Chem. Soc.* **2005**, 127, 1644–1645. (h) Kleij, A. W.; Lutz, M.; Spek, A. L.; van Leeuwen, P. W. N. M.; Reek, J. N. H. *Chem. Commun.* **2005**, 3661–3663. (i) Yoon, I.; Goto, M.; Shimizu, T.; Lee, S. S.; Asakawa, M. *Dalton Trans.* **2004**, 1513–1515. (j) Yoon, I.; Narita, M.; Shimizu, T.; Asakawa, M. *J. Am. Chem. Soc.* **2004**, 126, 16740–16741.
- (7) (a) Mizuno, T.; Takeuchi, M.; Shinkai, S. *Tetrahedron* **1999**, 55, 9455–9468. (b) Mizuno, T.; Yamamoto, M.; Takeuchi, M.; Shinkai, S. *Tetrahedron* **2000**, 56, 6193–6198.

Scheme 1. Principle of Cooperative Complexation of Bis(salamo) Ligand H₄L with Three d-Block Transition-Metal Ions

We have recently reported the acyclic bis(N₂O₂)-type ligand H₄L,¹⁵ in which two salamo^{16,17} chelate moieties share one benzene ring. When the two salamo moieties are metalated with d-block transition metals, the conformation of the molecules is restricted so that the phenoxo oxygen atoms are directed inward to form an O₆ cavity (Scheme 1).

The complexation of H₄L with zinc(II) acetate took place in a cooperative fashion and produced the homotrimeric complex [LZn₃]²⁺, in which the third zinc is in the O₆ cavity.¹⁵ This O₆ cavity is also utilized as an ion recognition site based on transmetalation, which leads to a novel helical heteronuclear metalloarchitecture having metallohost–guest components.^{15,18} These features mainly originate from the intrinsic properties of the mononuclear complexes of the salen-type ligands with d-block transition metals. These complexes act as a “complex ligand”, which can coordinate through the negatively charged phenoxo groups to alkali,¹⁹ alkaline earth,²⁰ rare earth,²¹ and d-block transition^{22,23}

- (8) (a) Pilkington, N. H.; Robson, R. *Aust. J. Chem.* **1970**, *23*, 2225–2236. (b) Guerriero, P.; Tamburini, S.; Vigato, P. A. *Coord. Chem. Rev.* **1995**, *139*, 17–243. (c) Okawa, H.; Furutachi, H.; Fenton, D. E. *Coord. Chem. Rev.* **1998**, *174*, 51–75. (d) Vigato, P. A.; Tamburini, S. *Coord. Chem. Rev.* **2004**, *248*, 1717–2128.
- (9) (a) van Veggel, F. C. J. M.; Bos, M.; Harkema, S.; Verboom, W.; Reinhoudt, D. N. *Angew. Chem., Int. Ed. Engl.* **1989**, *28*, 746–748. (b) van Veggel, F. C. J. M.; Bos, M.; Harkema, S.; van de Bovenkamp, H.; Verboom, W.; Reedijk, J.; Reinhoudt, D. N. *J. Org. Chem.* **1991**, *56*, 225–235. (c) Shimakoshi, H.; Takemoto, H.; Aritome, I.; Hisaeda, Y. *Tetrahedron Lett.* **2002**, *43*, 4809–4812. (d) Shimakoshi, H.; Takemoto, T.; Aritome, I.; Hisaeda, Y. *Inorg. Chem.* **2005**, *44*, 9134–9136.
- (10) (a) Pérez, M. A.; Bermejo, J. M. *J. Org. Chem.* **1993**, *58*, 2628–2630. (b) Houjou, H.; Lee, S.-K.; Hishikawa, Y.; Nagawa, Y.; Hiratani, K. *Chem. Commun.* **2000**, 2197–2198. (c) Fontecha, J. B.; Goetz, S.; McKee, V. *Dalton Trans.* **2005**, 923–929.
- (11) (a) Li, Z.; Jablonski, C. *Chem. Commun.* **1999**, 1531–1532. (b) Li, Z.; Jablonski, C. *Inorg. Chem.* **2000**, *39*, 2456–2461.
- (12) (a) Huck, W. T. S.; van Veggel, F. C. J. M.; Reinhoudt, D. N. *Recl. Trav. Chim. Pays-Bas* **1995**, *114*, 273–276. (b) Akine, S.; Taniguchi, T.; Nabeshima, T. *Tetrahedron Lett.* **2001**, *42*, 8861–8864. (c) Gallant, A. J.; MacLachlan, M. J. *Angew. Chem., Int. Ed.* **2003**, *42*, 5307–5310. (d) Akine, S.; Hashimoto, D.; Saiki, T.; Nabeshima, T. *Tetrahedron Lett.* **2004**, *45*, 4225–4227. (e) Nabeshima, T.; Miyazaki, H.; Iwasaki, A.; Akine, S.; Saiki, T.; Ikeda, C.; Sato, S. *Chem. Lett.* **2006**, *35*, 1070–1071. (f) Nabeshima, T.; Miyazaki, H.; Iwasaki, A.; Akine, S.; Saiki, T.; Ikeda, C. *Tetrahedron* **2007**, *63*, 3328–3333. (g) Akine, S.; Sunaga, S.; Taniguchi, T.; Miyazaki, H.; Nabeshima, T. *Inorg. Chem.* **2007**, *46*, 2959–2961.
- (13) (a) Konsler, R. G.; Karl, J.; Jacobsen, E. N. *J. Am. Chem. Soc.* **1998**, *120*, 10780–10781. (b) Shimakoshi, H.; Goto, A.; Tachi, Y.; Naruta, Y.; Hisaeda, Y. *Tetrahedron Lett.* **2001**, *42*, 1949–1951. (c) Shimakoshi, H.; Ninomiya, W.; Hisaeda, Y. *J. Chem. Soc., Dalton Trans.* **2001**, 1971–1974. (d) Shimakoshi, H.; Kaieda, T.; Matsuo, T.; Sato, H.; Hisaeda, Y. *Tetrahedron Lett.* **2003**, *44*, 5197–5199.
- (14) (a) Ready, J. M.; Jacobsen, E. N. *J. Am. Chem. Soc.* **2001**, *123*, 2687–2688. (b) Ready, J. M.; Jacobsen, E. N. *Angew. Chem., Int. Ed.* **2002**, *41*, 1374–1377.
- (15) (a) Akine, S.; Taniguchi, T.; Nabeshima, T. *Angew. Chem., Int. Ed.* **2002**, *41*, 4670–4673. (b) Akine, S.; Taniguchi, T.; Saiki, T.; Nabeshima, T. *J. Am. Chem. Soc.* **2005**, *127*, 540–541. (c) Akine, S.; Matsumoto, T.; Taniguchi, T.; Nabeshima, T. *Inorg. Chem.* **2005**, *44*, 3270–3274. (d) Akine, S.; Taniguchi, T.; Nabeshima, T. *J. Am. Chem. Soc.* **2006**, *128*, 15765–15774. (e) Akine, S.; Kagiya, S.; Nabeshima, T. *Inorg. Chem.* **2007**, *46*, 9525–9527.
- (16) H₂salamo = 1,2-bis(salicylideneaminoxy)ethane. See: (a) Akine, S.; Taniguchi, T.; Nabeshima, T. *Chem. Lett.* **2001**, 682–683. (b) Akine, S.; Taniguchi, T.; Dong, W.; Masubuchi, S.; Nabeshima, T. *J. Org. Chem.* **2005**, *70*, 1704–1711.
- (17) For related salamo complexes, see: (a) Akine, S.; Taniguchi, T.; Nabeshima, T. *Inorg. Chem.* **2004**, *43*, 6142–6144. (b) Akine, S.; Nabeshima, T. *Inorg. Chem.* **2005**, *44*, 1205–1207. (c) Akine, S.; Taniguchi, T.; Nabeshima, T. *Chem. Lett.* **2006**, *35*, 604–605. (d) Akine, S.; Dong, W.; Nabeshima, T. *Inorg. Chem.* **2006**, *45*, 4677–4684.
- (18) Akine, S.; Taniguchi, T.; Matsumoto, T.; Nabeshima, T. *Chem. Commun.* **2006**, 4961–4963.
- (19) (a) Armstrong, L. G.; Lip, H. C.; Lindoy, L. F.; McPartlin, M.; Tasker, P. A. *J. Chem. Soc., Dalton Trans.* **1977**, 1771–1774. (b) Giacomelli, A.; Rotunno, T.; Senatore, L. *Inorg. Chem.* **1985**, *24*, 1303–1306. (c) Giacomelli, A.; Rotunno, T.; Senatore, L.; Settambolo, R. *Inorg. Chem.* **1989**, *28*, 3552–3555. (d) Cunningham, D.; McArdle, P.; Mitchell, M.; Ní Chonchubhair, N.; O’Gara, M.; Franceschi, F.; Floriani, C. *Inorg. Chem.* **2000**, *39*, 1639–1649.
- (20) Carbonaro, L.; Isola, M.; La Pegna, P.; Senatore, L.; Marchetti, F. *Inorg. Chem.* **1999**, *38*, 5519–5525.
- (21) (a) Condorelli, G.; Fragalà, I.; Giuffrida, S.; Cassol, A. Z. *Anorg. Allg. Chem.* **1975**, *412*, 251–257. (b) Costisor, O.; Linert, W. *Rev. Inorg. Chem.* **2005**, *25*, 13–54.
- (22) For homometal systems, see: (a) Bear, C. A.; Waters, J. M.; Waters, T. N. *J. Chem. Soc., Dalton Trans.* **1974**, 1059–1062. (b) Epstein, J. M.; Figgis, B. N.; White, A. H.; Willis, A. C. *J. Chem. Soc., Dalton Trans.* **1974**, 1954–1961. (c) Leslie, K. A.; Drago, R. S.; Stucky, G. D.; Kitko, D. J.; Breese, J. A. *Inorg. Chem.* **1979**, *18*, 1885–1891. (d) Fukuhara, C.; Asato, E.; Shimoji, T.; Katsura, K.; Mori, M.; Matsumoto, K.; Ooi, S. *J. Chem. Soc., Dalton Trans.* **1987**, 1305–1311. (e) Fukuhara, C.; Tsuneyoshi, K.; Katsura, K.; Matsumoto, N.; Kida, S.; Mori, M. *Bull. Chem. Soc. Jpn.* **1989**, *62*, 3939–3943. (f) Cunningham, D.; Gallagher, J. F.; Higgins, T.; McArdle, P.; McGinley, J.; Sheerin, D. *J. Chem. Soc., Chem. Commun.* **1990**, 959–961. (g) Gerli, A.; Hagen, K. S.; Marzilli, L. G. *Inorg. Chem.* **1991**, *30*, 4673–4676. (h) Cacelli, I.; Carbonaro, L.; La Pegna, P. *Eur. J. Inorg. Chem.* **2002**, 1703–1710. (i) Ülkü, D.; Ercan, F.; Atakol, O.; Dinçer, F. N. *Acta Crystallogr.* **1997**, *C53*, 1056–1057. (j) Atakol, O.; Arici, C.; Ercan, F.; Ülkü, D. *Acta Crystallogr.* **1999**, *C55*, 511–513. (k) Atakol, O.; Aksu, M.; Ercan, F.; Arici, C.; Tahir, M. N.; Ülkü, D. *Acta Crystallogr.* **1999**, *C55*, 1072–1075. (l) Zhang, L.; Jones, R. A.; Lynch, V. M. *Chem. Commun.* **2002**, 2986–2987. (m) Reglinski, J.; Morris, S.; Stevenson, D. E. *Polyhedron* **2002**, *21*, 2167–2174. (n) Reglinski, J.; Morris, S.; Stevenson, D. E. *Polyhedron* **2002**, *21*, 2175–2182.
- (23) For heterometal systems, see: (a) Gruber, S. J.; Harris, C. M.; Sinn, E. *J. Inorg. Nucl. Chem.* **1968**, *30*, 1805–1830. (b) O’Bryan, N. B.; Maier, T. O.; Paul, I. C.; Drago, R. S. *J. Am. Chem. Soc.* **1973**, *95*, 6640–6645. (c) Fukuhara, C.; Tsuneyoshi, K.; Matsumoto, N.; Kida, S.; Mikuriya, M.; Mori, M. *J. Chem. Soc., Dalton Trans.* **1990**, 3473–3479. (d) Ülkü, D.; Tahir, M. N.; Atakol, O.; Nazir, H. *Acta Crystallogr.* **1997**, *C53*, 872–874. (e) Tahir, M. N.; Ülkü, D.; Atakol, O.; Çakirer, O. *Acta Crystallogr.* **1998**, *C54*, 468–470. (f) Ercan, F.; Atakol, O. *Acta Crystallogr.* **1998**, *C54*, 1268–1270. (g) Ercan, F.; Ülkü, D.; Atakol, O.; Dinçer, F. N. *Acta Crystallogr.* **1998**, *C54*, 1787–1790. (h) Ülkü, D.; Tatar, L.; Atakol, O.; Durmus, S. *Acta Crystallogr.* **1999**, *C55*, 1652–1654.

Table 1. Crystallographic Data for Trinuclear Complexes

	H ₄ L	[LMn ₃ (OAc) ₂ (MeOH) ₂]	[LCo ₃ (OAc) ₂ (EtOH) ₂]·2CHCl ₃	[LZn ₂ Mn(OAc) ₂ (MeOH) ₂]	[LCu ₂ Zn(OAc) ₂ (H ₂ O)]·MeOH·8.5H ₂ O
cryst syst	monoclinic	triclinic	triclinic	triclinic	triclinic
space group	<i>Pn</i>	<i>P</i> $\bar{1}$	<i>P</i> $\bar{1}$	<i>P</i> $\bar{1}$	<i>P</i> $\bar{1}$
<i>a</i> /Å	4.5616(7)	9.584(6)	13.291(6)	11.168(5)	12.961(9)
<i>b</i> /Å	37.891(5)	13.666(9)	13.913(7)	12.914(6)	14.588(11)
<i>c</i> /Å	7.9858(11)	15.566(10)	14.599(8)	15.231(5)	14.682(11)
α /deg		108.702(8)	88.27(2)	68.539(16)	111.177(7)
β /deg	101.373(2)	95.255(4)	67.391(15)	68.930(16)	109.929(6)
γ /deg		101.023(8)	73.90(2)	86.77(2)	96.218(7)
<i>V</i> /Å ³	1353.2(3)	1870(2)	2386(2)	1900.6(13)	2347(3)
<i>Z</i>	2	2	2	2	2
<i>D</i> _{calc} /g cm ⁻³	1.430	1.644	1.677	1.654	1.545
<i>T</i> /K	90	120	120	150	120
<i>R</i> ¹ [<i>I</i> > 2σ(<i>I</i>)]	0.0623	0.0405	0.0778	0.0449	0.0855
w <i>R</i> ² (all data)	0.1266	0.1012	0.1763	0.1166	0.2431

$$^a R1 = \sum ||F_o| - |F_c|| / \sum |F_o|; wR2 = [\sum (w(F_o^2 - F_c^2)^2) / \sum (w(F_o^2)^2)]^{1/2}.$$

metals. Such μ_2 -phenoxo bridging is particularly important for the d-block homo- and heterometal complexes of compartmental ligands, some of which exhibit interesting electrochemical and magnetic properties. In this report, we describe the complexation of the acyclic bis(N₂O₂) ligand H₄L with d-block transition metals (Mn^{II}, Co^{II}, Ni^{II}, and Cu^{II}). The homotrimeric d-block metal complexes [LCo₃(OAc)₂(EtOH)₂] and [LMn₃(OAc)₂(MeOH)₂] were easily obtained, and the structures were determined by X-ray crystallography. The synthesis of some heterotrimeric d-block metal complexes was also achieved by the site-selective metalation of the N₂O₂ and O₆ sites with two different d-block transition metals.

Experimental Section

General Procedures. All experiments were carried out in air. Ligand H₄L was prepared according to the procedures reported previously.^{15d} Commercial chloroform, methanol, and ethanol were used without purification. All chemicals were of reagent grade and were used as received.

Synthesis of Manganese(II) Complex [LMn₃(OAc)₂]. A solution of manganese(II) acetate tetrahydrate (7.4 mg, 0.030 mmol) in methanol (8 mL) was added to a solution of ligand H₄L (5.8 mg, 0.010 mmol) in chloroform/methanol (1:2, 3 mL). The resulting solution was concentrated to dryness, and the residue was recrystallized from chloroform/methanol/ether to afford [LMn₃(OAc)₂] (6.7 mg, 72%) as brown crystals. Anal. Calcd for C₃₂H₃₂Mn₃N₄O₁₄·2MeOH: C, 44.12; H, 4.36; N, 6.05. Found: C, 43.61; H, 4.38; N, 5.89.

Synthesis of Cobalt(II) Complex [LCo₃(OAc)₂]. A hot solution of cobalt(II) acetate tetrahydrate (29.9 mg, 0.12 mmol) in ethanol (10 mL) was added to a solution of ligand H₄L (23.3 mg, 0.040 mmol) in chloroform/ethanol (1:4, 10 mL). After the resulting solution was allowed to stand at room temperature, the precipitates were collected to give [LCo₃(OAc)₂] (26.7 mg, 64%) as brown crystals. Anal. Calcd for C₃₂H₃₂Co₃N₄O₁₄·0.5EtOH·1.5H₂O·CHCl₃: C, 39.16; H, 3.77; N, 5.37. Found: C, 39.01; H, 4.06; N, 5.58.

Synthesis of Nickel(II) Complex [LNi₃(OAc)₂]. A solution of nickel(II) acetate tetrahydrate (7.5 mg, 0.030 mmol) in methanol (1 mL) was added to a solution of ligand H₄L (5.8 mg, 0.010 mmol) in dichloromethane (1 mL). The resulting solution was concentrated to dryness, and the residue was recrystallized from chloroform/ether to afford [LNi₃(OAc)₂] (6.7 mg, 68%) as yellow crystals. Anal.

Calcd for C₃₂H₃₂N₄Ni₃O₁₄·2MeOH·3H₂O: C, 41.21; H, 4.68; N, 5.65. Found: C, 41.02; H, 4.28; N, 5.45.

Synthesis of Zinc(II)–Manganese(II) Complex [LZn₂Mn(OAc)₂]. Solutions of zinc(II) acetate dihydrate (4.4 mg, 0.020 mmol) in methanol (1 mL) and manganese(II) acetate tetrahydrate (2.5 mg, 0.010 mmol) in methanol (1 mL) were added to a solution of ligand H₄L (5.8 mg, 0.010 mmol) in chloroform (2 mL). The resulting solution was concentrated to dryness, and the residue was recrystallized from chloroform/methanol/ether to afford [LZn₂Mn(OAc)₂] (8.9 mg, 95%) as yellow crystals. Anal. Calcd for C₃₂H₃₂MnN₄O₁₄Zn₂·MeOH·H₂O: C, 42.51; H, 4.11; N, 6.01. Found: C, 42.54; H, 3.93; N, 5.79.

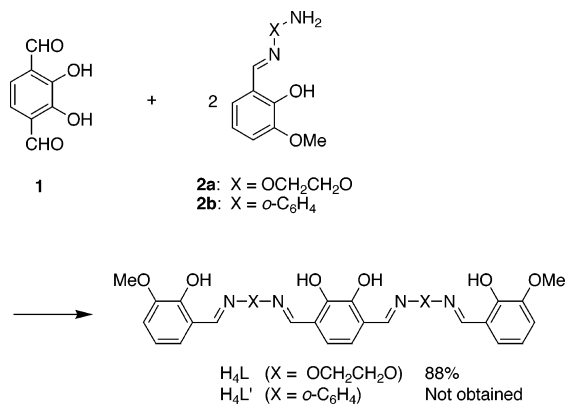
Synthesis of Copper(II)–Zinc(II) Complex [LCu₂Zn(OAc)₂]. Solutions of copper(II) acetate hydrate (4.0 mg, 0.020 mmol) in methanol (1 mL) and zinc(II) acetate dihydrate (2.2 mg, 0.010 mmol) in methanol (1 mL) were added to a solution of ligand H₄L (5.8 mg, 0.010 mmol) in chloroform (2 mL). The resulting solution was concentrated to dryness, and the residue was recrystallized from chloroform/methanol/ether to afford [LCu₂Zn(OAc)₂] (8.4 mg, 91%) as dark-brown crystals. Anal. Calcd for C₃₂H₃₂Cu₂N₄O₁₄Zn·2H₂O: C, 41.54; H, 3.92; N, 6.06. Found: C, 41.49; H, 4.21; N, 5.54.

Spectrophotometric Titration. Sample solutions containing H₄L (2.0 × 10⁻⁴ M) and varying amounts of M(OAc)₂ (M = Mn^{II}, Co^{II}, Ni^{II}, and Cu^{II}; 0–5 equiv) in chloroform/methanol (1:1, 5 mL) were prepared. Spectra were recorded at ambient temperature in a 1-mm-path-length quartz cell on a Jasco V560 or V570 spectrophotometer.

Mass Spectrometry. Sample solutions containing H₄L (1.0 × 10⁻⁵ M) and MX₂ (M = Mn^{II}, Co^{II}, Ni^{II}, and Cu^{II}; X = OAc or Cl; 3.0 × 10⁻⁵ M for each) in chloroform/methanol (1:1) were prepared. In the measurements for heterometal complexes, sample solutions containing H₄L and two kinds of M(OAc)₂ (M = Mn^{II}, Co^{II}, Ni^{II}, Cu^{II}, and Zn^{II}) were prepared. Mass spectra (electrospray ionization time-of-flight, ESI-TOF, positive mode) were recorded on an Applied Biosystems QStar Pulsar *i* spectrometer.

X-ray Crystallographic Analysis. Intensity data were collected on a Bruker APEX II CCD, a Rigaku Mercury CCD, or a Rigaku R-Axis Rapid diffractometer with Mo K α radiation ($\lambda = 0.710$ 69 Å). Reflection data were corrected for Lorentz and polarization factors and for absorption using the multiscan method. Crystallographic data are summarized in Table 1. The structures were solved by direct methods (*SIR 97*)²⁴ or Patterson methods (*DIREDF*

(24) *SIR 97, program for crystal structure solution*: Altomare, A.; Burla, M. C.; Camalli, M.; Casciarano, G. L.; Giacovazzo, C.; Guagliardi, A.; Moliterni, A. G. G.; Polidori, G.; Spagna, R. *J. Appl. Crystallogr.* **1999**, *32*, 115–119.

Scheme 2. Synthesis of Bis(N₂O₂ chelate) Ligands

99)²⁵ and refined by full-matrix least squares on F^2 using *SHELXL* 97.²⁶ The non-hydrogen atoms were refined anisotropically except for some disordered atoms. Hydrogen atoms were included at idealized positions refined by use of the riding models.

Results and Discussion

Synthesis and Crystal Structure of the Free Ligand H₄L. The ligand H₄L was prepared by the reaction of the oxime **2a** with 2,3-dihydroxybenzene-1,4-dicarbaldehyde (**1**).^{15d} In a similar manner, we also attempted the synthesis of the bis(H₂saloph) ligand H₄L', which contained imine moieties instead of the oxime (Scheme 2). The monoimine **2b**²⁷ was obtained in 78% yield by the reaction of 2-hydroxy-3-methoxybenzaldehyde with 2 equiv of *o*-phenylenediamine in ethanol. From the reaction mixture of the monoimine **2b** and 0.5 equiv of the dialdehyde **1** in acetonitrile, a dark-red crystalline product precipitated. However, the product was identified as the macrocyclic tris(H₂saloph) **3**^{12b} (Chart 1) instead of the desired acyclic bis(H₂saloph) ligand H₄L'. In addition, the H₂saloph derivative **4** was also detected in the ¹H NMR spectrum of the reaction mixture. Undoubtedly, these two compounds are derived from the C=N bond recombination.²⁸ The extremely low solubility of the macrocycle **3** may shift the equilibrium to the formation of **3**.^{12b} Thus, we concluded that an imine group²⁹ is not suitable as a constituent of the acyclic bis(N₂O₂ chelate) ligands.

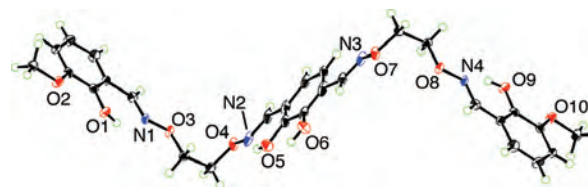
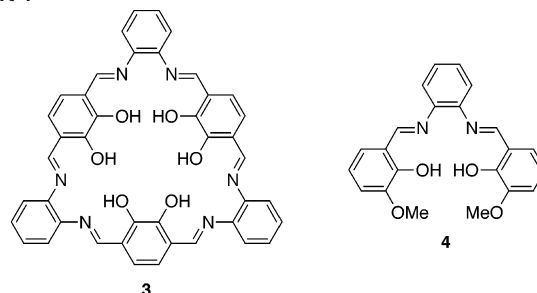


Figure 1. Crystal structure of bis(salamo) ligand H₄L with thermal ellipsoids plotted at the 50% probability level.

Chart 1



We reported that H₂salamo [=1,2-bis(salicylideneaminoxy)ethane, an *O*-alkyloxime analogue of H₂salen] derivatives are highly stable under conditions in which the imine analogues suffer from the C=N recombination.^{16,17} The synthetic intermediate monooxime **2a** and the target tetraoxime ligand H₄L were sufficiently stable to resist such a C=N bond recombination.

The crystal structure of H₄L was determined by X-ray crystallography (Figure 1). The molecule adopts a zigzag conformation where the two salicyldoxime moieties are separated from each other. Probably, packing effects account for the zigzag conformation in the crystalline state. Three hydroxyl groups (O1, O5, and O9) are involved in the O—H···N hydrogen bond to the oxime nitrogen, whereas O6 forms an O—H···O hydrogen bond. The corresponding oxime nitrogen (N3) is located in the direction opposite to the phenol oxygen (O6).

Complexation of H₄L with Manganese(II), Cobalt(II), Nickel(II), and Copper(II). We have already reported that the complexation of the ligand H₄L with zinc(II) acetate takes place in a cooperative fashion to give the homotrimeric complex [LZn₃]²⁺.^{15a,d} The corresponding trinuclear complexes having paramagnetic metals, such as manganese(II) and cobalt(II), are interesting from the viewpoint of the electrochemical or magnetic properties.³⁰ Thus, we investigated the complexation of H₄L with manganese(II), cobalt(II), nickel(II), and copper(II) by spectroscopic methods in a similar manner.

The color of a solution of H₄L in chloroform/methanol (1:1) immediately changed from colorless to yellow upon the addition of a solution of cobalt(II) acetate. Two bands at 304 and 317 nm disappeared and a new band at 345 nm appeared in the absorption spectrum (Figure 2b). As in the case of the zinc(II) complex,^{15a,d} the spectroscopic titration clearly indicates the formation of a 1:3 complex, although

(25) Beurskens, P. T.; Beurskens, G.; de Gelder, R.; Garcia-Granda, S.; Gould, R. O.; Israel R.; Smits, J. M. M. *The DIRDIF 99 program system*; Crystallography Laboratory, University of Nijmegen: Nijmegen, The Netherlands, 1999.

(26) Sheldrick, G. M. *SHELXL 97, Program for crystal structure refinement*; University of Göttingen: Göttingen, Germany, 1997.

(27) Sasaki, I.; Pujol, D.; Gaudemer, A. *Inorg. Chim. Acta* **1987**, *134*, 53–57.

(28) Similar C=N bond recombination affords a macrocyclic imine. See: Houjou, H.; Nagawa, Y.; Hiratani, K. *Tetrahedron Lett.* **2001**, *42*, 3861–3863.

(29) We also attempted the synthesis of the bis(H₂salen) ligand; however, we could not purify the monoimine precursor analogous to **2a**, probably because of the C=N recombination.

(30) (a) Ama, T.; Rashid, M. M.; Yonemura, T.; Kawaguchi, H.; Yasui, T. *Coord. Chem. Rev.* **2000**, *198*, 101–116. (b) Winpenny, R. E. P. *J. Chem. Soc., Dalton Trans.* **2002**, 1–10. (c) Laye, R. H.; McInnes, E. J. L. *Eur. J. Inorg. Chem.* **2004**, 2811–2818. (d) Christou, G. *Polyhedron* **2005**, *24*, 2065–2075.

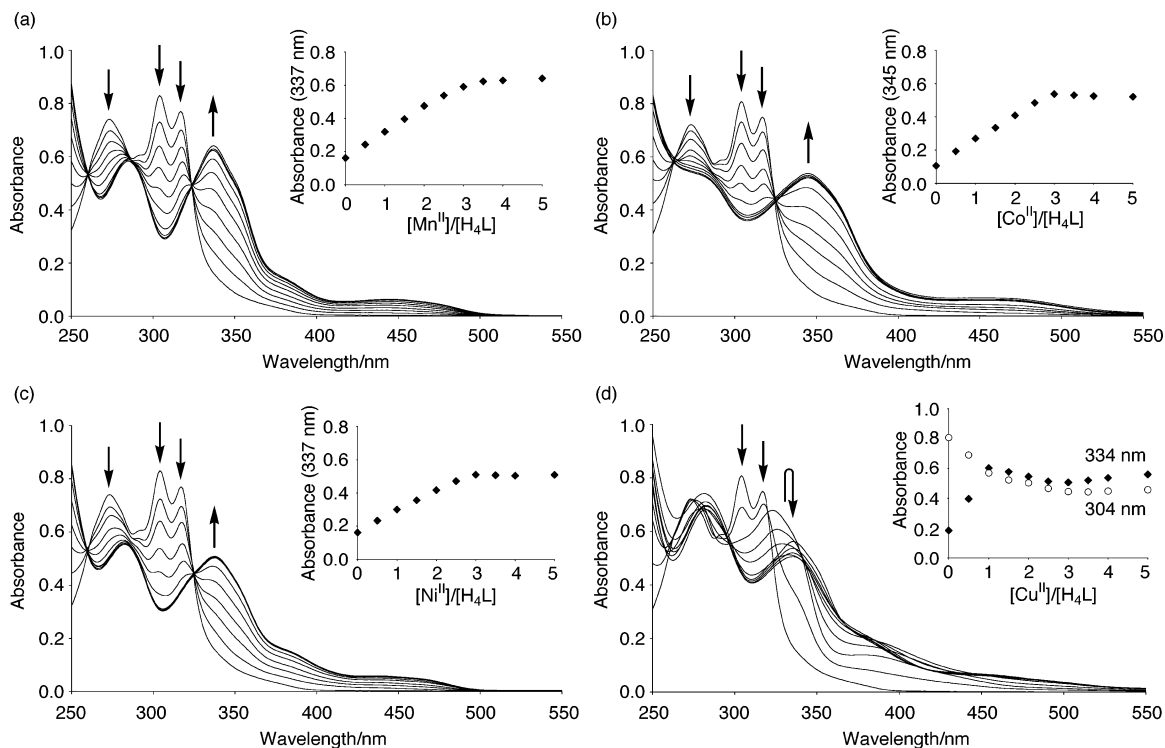


Figure 2. UV-vis spectral changes of H_4L by the addition of $M(OAc)_2$ ($CHCl_3/CH_3OH$ (1:1), $[H_4L] = 2.0 \times 10^{-4}$ M): (a) $M = Mn^{II}$; (b) $M = Co^{II}$; (c) $M = Ni^{II}$; (d) $M = Cu^{II}$. The inset shows the plot of absorbance at 337 nm (Mn^{II} and Ni^{II}), 345 nm (Co^{II}), and 304 and 334 nm (Cu^{II}) versus the molar ratio $[M^{II}]/[H_4L]$.

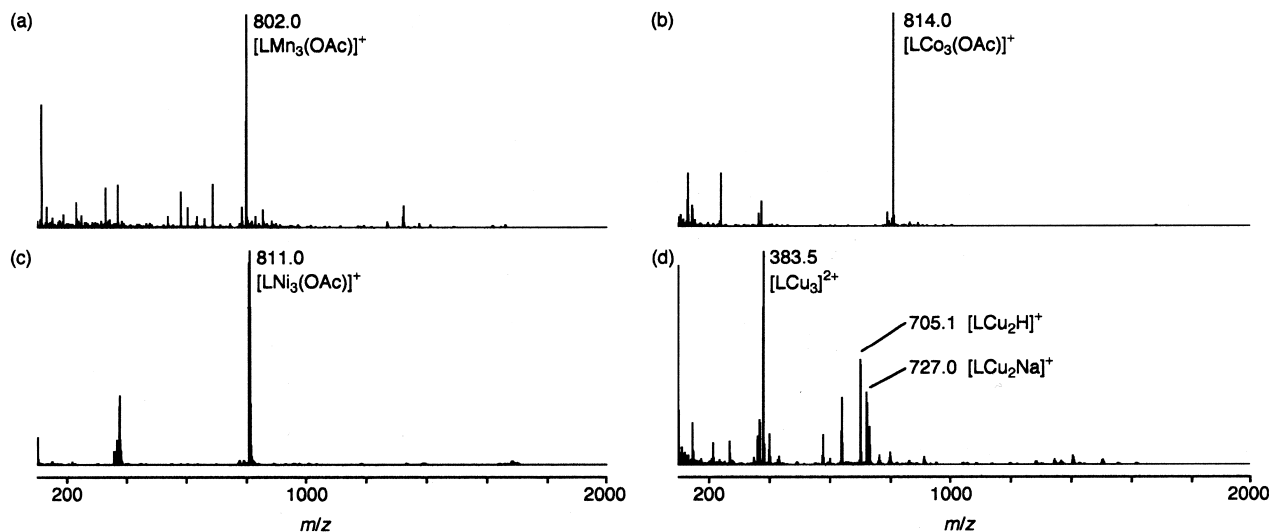


Figure 3. ESI mass spectra of H_4L in the presence of $M(OAc)_2$ (3 equiv): (a) $M = Mn^{II}$; (b) $M = Co^{II}$; (c) $M = Ni^{II}$; (d) $M = Cu^{II}$.

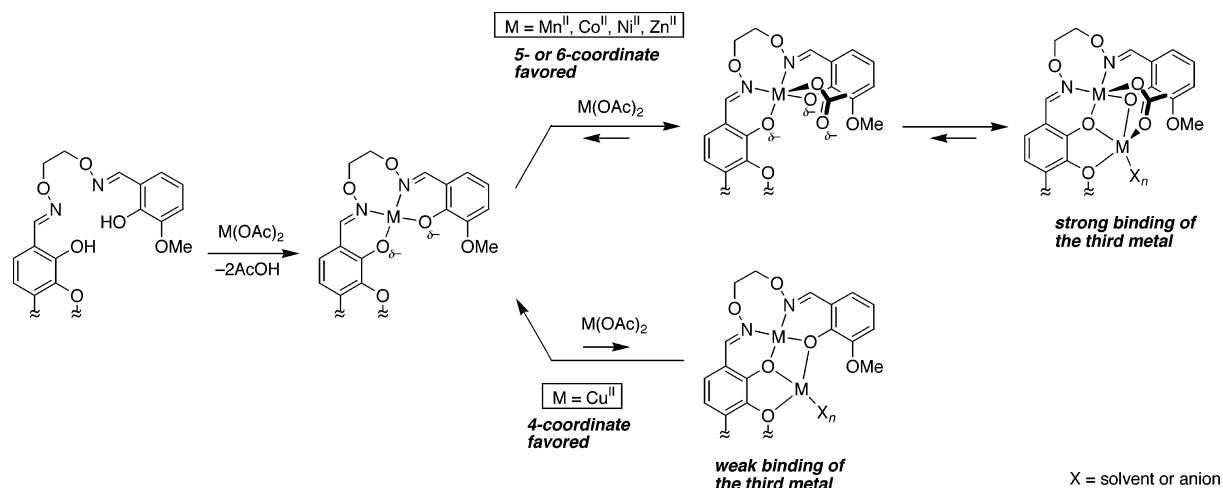
the ligand H_4L has two salamo chelate moieties. The exclusive and cooperative formation of the 1:3 complex was suggested by the spectral changes because the isosbestic points (263 and 325 nm) were observed when up to 3 equiv of cobalt(II) was added. The titration experiments also showed a similar 1:3 complexation of H_4L with manganese(II) and nickel(II) (Figure 2a,c). In general, the cobalt(II) and manganese(II) complexes of the salen-type Schiff base ligands are readily oxidized when exposed to air.^{12f,31} This process can be easily monitored by the change in the absorption spectra. In the case of the oxime-based ligand H_4L , however, such a spectral change due to autoxidation was not observed. Thus, the 1:3 complexes of H_4L with

cobalt(II) or manganese(II) was proven to be stable under aerobic conditions.

In the ESI mass spectra, strong peaks for $[LM_3(OAc)]^+$ ($M = Mn^{II}$, m/z 802.0; $M = Co^{II}$, m/z 814.0; $M = Ni^{II}$, m/z 811.0) were observed (Figure 3a–c). These peaks clearly indicated the existence of trinuclear complexes similar to the zinc(II) complex.^{15a,d} It is important to note that these ions observed in the mass spectra contain an acetato ligand.

(31) (a) Biswas, S.; Mitra, K.; Schwalbe, C. H.; Lucas, C. R.; Chattopadhyay, S. K.; Adhikary, B. *Inorg. Chim. Acta* **2005**, *358*, 2473–2481. (b) Amirnasr, M.; Schenk, K. J.; Gorji, A.; Vafazadeh, R. *Polyhedron* **2001**, *20*, 695–702.

Scheme 3. Plausible Mechanism for the Formation of Trinuclear Complexes



The acetate ion should play an important role in the cooperative formation of the trinuclear complexes. As described above, the reaction of H_4L with $\text{M}(\text{OAc})_2$ ($M = \text{Mn}^{\text{II}}, \text{Co}^{\text{II}}, \text{Ni}^{\text{II}}$) resulted in the cooperative formation of $[\text{LM}_3]^{2+}$, and the acetate ion is strongly bound to the trinuclear core in solution as in the crystalline state (vide infra). The acetate adduct formation may be favorable when the metal ions prefer the penta- and hexacoordinate environments (Scheme 3). Indeed, manganese(II), cobalt(II) (vide infra), nickel(II),^{17b} and zinc(II)^{17a} in an N_2O_2 salamo chelate site are penta- or hexacoordinate with additional coordination of anions or solvent molecules. The acetate ion, which is strongly bound to the metal in the salamo site, attracts the third metal ion in the central O_6 site by forming a μ_2 -acetato bridge (vide infra).

Interestingly, no cooperative 1:3 complexation was observed when H_4L was titrated with copper(II) acetate. The addition of 1 equiv of copper(II) caused a new peak at 323 nm, but the intensity of the peak became low and the peak shifted to a longer wavelength when more than 1 equiv of copper(II) was added (Figure 2d). The stoichiometry of the copper(II) complex was not reliably determined by a molar

ratio plot of the titration experiments. Because there are no isosbestic points observed in the spectra, two or more complexes, such as the di- and trinuclear ones, are suggested to form in a stepwise fashion.

In the ESI mass spectrum of H_4L in the presence of 3 equiv of copper(II) acetate, both the di- and trinuclear complexes were detected (Figure 3d). The dinuclear species was observed as $[\text{LCu}_2\text{H}]^+$ (m/z 705.1) and $[\text{LCu}_2\text{Na}]^+$ (m/z 727.0), indicating that there is a considerable amount of the dinuclear complex $[\text{LCu}_2]$ in solution even in the presence of excess copper(II) acetate. In addition, the trinuclear complex was observed as a dicationic species $[\text{LCu}_3]^{2+}$ (m/z 383.5). It is noteworthy that the peak intensity for the acetate adduct $[\text{LCu}_3(\text{OAc})]^+$ was low. This observation strongly indicates the weak coordination of the acetate ion to $[\text{LCu}_3]^{2+}$.

The reason why the complexation behavior of H_4L with copper(II) is different from that with other metals can be explained as follows. Salamo-type ligands can form stable tetracoordinate complexes with copper(II),^{15c,16a} whereas penta- or hexacoordinate ones form with other metals ($\text{Mn}^{\text{II}}, \text{Co}^{\text{II}}, \text{Ni}^{\text{II}}, \text{and Zn}^{\text{II}}$). The additional coordination of the acetate

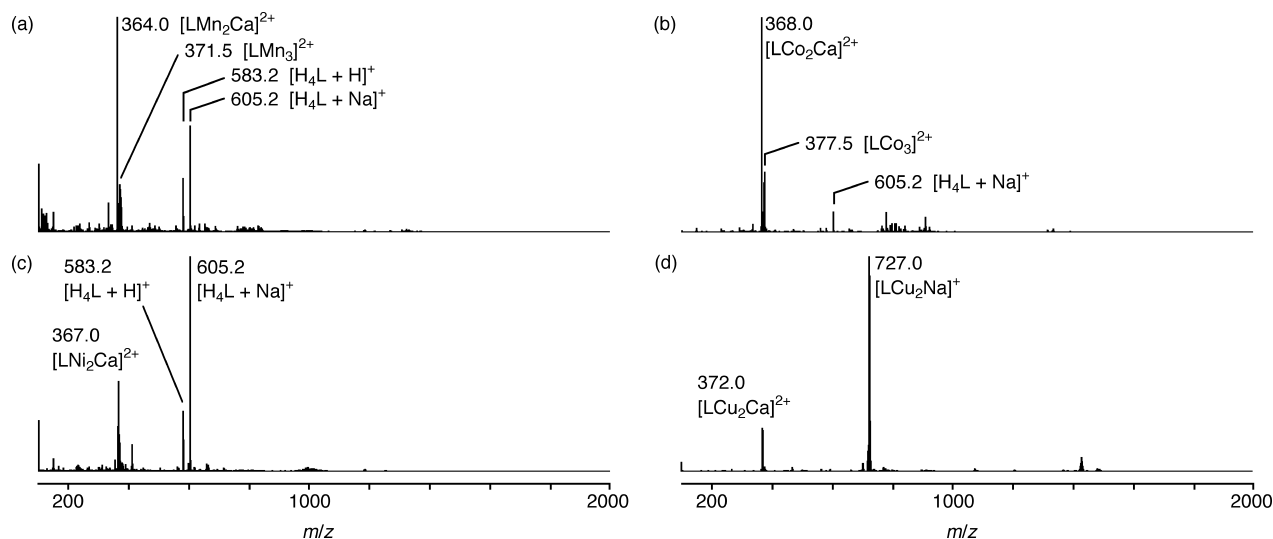


Figure 4. ESI mass spectra of H_4L in the presence of MCl_2 (3 equiv): (a) $M = \text{Mn}^{\text{II}}$; (b) $M = \text{Co}^{\text{II}}$; (c) $M = \text{Ni}^{\text{II}}$; (d) $M = \text{Cu}^{\text{II}}$.

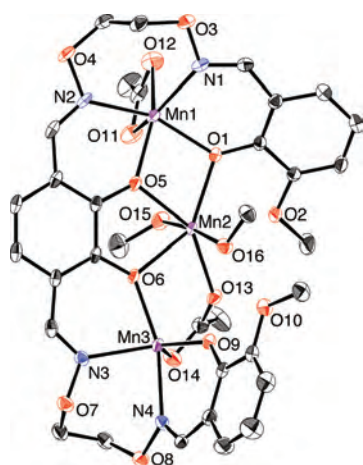


Figure 5. Crystal structure of $[LMn_3(OAc)_2(MeOH)_2]$ (ORTEP, 50% probability).

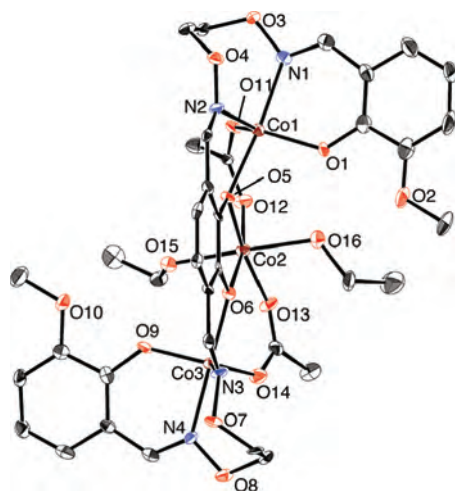


Figure 6. Crystal structure of $[LCo_3(OAc)_2(EtOH)_2]$ (ORTEP, 50% probability).

ion to copper(II) in the salamo site, which changes the copper(II) from tetra- to pentacoordinate, is not prone to take place. Because the coordination of the acetate ion is weak, the μ_2 -acetato bridging cannot enhance the interaction between the salamocopper(II) unit and the additional copper(II). Consequently, the complexation of $[LCu_2]$ with a third copper(II), which is mainly due to the μ_2 -phenoxo bridging, is less favored. This is in contrast to the manganese(II), cobalt(II), and nickel(II) systems, in which the acetate ion is strongly bound to the trinuclear core. Thus, we again confirmed that the bridging μ_2 -acetato ligand plays an important role in the strong binding of $[LM_2]$ toward the third M^{II} , which causes the cooperative formation of the trinuclear complexes $[LM_3]^{2+}$.

To confirm the effect of the acetate ion on stabilization of the $[LM_3]^{2+}$ species, complexation of H_4L with metal ions was studied in the absence of the acetate ion. The ESI mass spectra of H_4L in the presence of MCl_2 ($M = Mn^{II}$, Co^{II} , and Ni^{II} ; Figure 4a–c) clearly indicated the existence of dinuclear species $[LM_2]$, which was confirmed by the peaks for $[LM_2Ca]^{2+}$ (m/z 364.0 for $M = Mn^{II}$; m/z 368.0 for $M = Co^{II}$; m/z 367.0 for $M = Ni^{II}$). Trinuclear species $[LM_3]^{2+}$ was also detected for $M = Mn^{II}$ (m/z 371.5) and $M = Co^{II}$

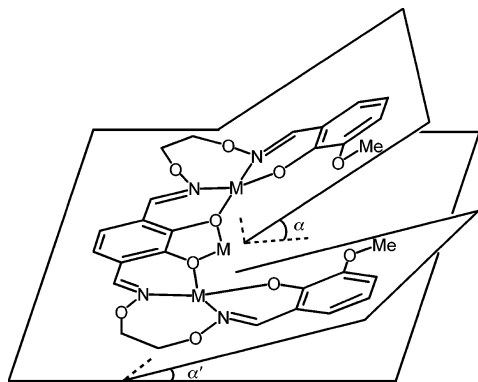
Table 2. Selected Interatomic Distances (Å) of Complexes $[LMn_3(OAc)_2(MeOH)_2]$ and $[LCo_3(OAc)_2(EtOH)_2]$

	$[LMn_3(OAc)_2(MeOH)_2]$	$[LCo_3(OAc)_2(EtOH)_2]$	
Mn1–N1	2.278(2)	Co1–N1	2.106(6)
Mn1–N2	2.267(2)	Co1–N2	2.062(6)
Mn1–O1	2.1063(19)	Co1–O1	1.938(4)
Mn1–O5	2.1081(19)	Co1–O5	2.060(5)
Mn1–O11	2.209(2)	Co1–O11	1.997(5)
Mn1–O12	2.348(2)		
Mn2–O1	2.2069(19)	Co2–O5	2.083(5)
Mn2–O2	2.589(2)	Co2–O6	2.039(5)
Mn2–O5	2.2003(18)	Co2–O12	2.061(5)
Mn2–O6	2.2552(19)	Co2–O13	2.049(5)
Mn2–O13	2.1800(19)	Co2–O15	2.156(5)
Mn2–O15	2.228(2)	Co2–O16	2.125(5)
Mn2–O16	2.173(2)		
Mn3–N3	2.268(2)	Co3–N3	2.056(6)
Mn3–N4	2.269(2)	Co3–N4	2.102(6)
Mn3–O6	2.0954(19)	Co3–O6	2.049(5)
Mn3–O9	2.0650(18)	Co3–O9	1.935(5)
Mn3–O14	2.163(2)	Co3–O14	2.012(5)

(m/z 377.5). In addition, peaks corresponding to the free ligand were observed as $[H_4L + H]^+$ (m/z 583.2) and $[H_4L + Na]^+$ (m/z 605.2). Obviously, trinuclear complex $[LM_3]^{2+}$ did not form efficiently under the conditions. Consequently, the acetate ion is essential for the efficient and cooperative formation of trinuclear complex $[LM_3]^{2+}$ ($M = Mn^{II}$, Co^{II} , and Ni^{II}). The mass spectrum of H_4L in the presence of $CuCl_2$ also showed peaks related to dinuclear species $[LCu_2Na]^+$ (m/z 727.0) and $[LCu_2Ca]^{2+}$ (m/z 372.0) (Figure 4d). In this case, however, peaks for trinuclear species $[LCu_3]^{2+}$ or free ligand H_4L were not detected. This result suggested that dinuclear complex $[LCu_2]$ was almost exclusively formed and that the formation of trinuclear complex $[LCu_3]^{2+}$ is less favored in the absence of acetate ion.

Crystal Structures of Manganese(II) and Cobalt(II) Complexes. An X-ray crystallographic analysis revealed that the manganese(II) complex consists of one ligand L^{4-} , three manganese(II) ions, two acetato ligands, and two methanol molecules (Figure 5 and Table 2). Mn1 and Mn3 sit in the N_2O_2 chelate sites. In addition, an acetato ligand coordinates to Mn1 having a distorted octahedral geometry in an η^2 fashion and another acetato ligand bridges Mn2 and Mn3. The geometry of Mn3 is trigonal-bipyramidal. On the other hand, Mn2 has a pentagonal-bipyramidal geometry with seven oxygen donors in which two methanol molecules occupy the axial positions (O15 and O16). The ligand L^{4-} coordinates to Mn2 through three phenoxo donors (O1, O5, and O6), with Mn2–O distances ranging from 2.200 to 2.255 Å. A weak coordination bond was also found between Mn2 and a methoxy group of ligand L^{4-} [Mn2–O2 2.589(2) Å]. Thus, the four oxygen donors in L^{4-} coordinate to Mn2, which forces the structure of the L^{4-} moiety into a C-shaped one. In the crystal structure, two methanol molecules are involved in the hydrogen bonding: one to the phenoxo oxygen [O16–O9 2.783(3) Å] and the other to the acetato oxygen [O15–O11, 2.629(3) Å]. These intramolecular hydrogen bonds may stabilize the trinuclear structure.

In contrast, the cobalt(II) complex has an S-shaped structure (Figure 6 and Table 2), although it has the composition $[LCo_3(OAc)_2(EtOH)_2]$ similar to the manganese(II) analogue. Two of the three cobalt atoms (Co1 and

Scheme 4. Dihedral Angles α and α' of Trinuclear Complexes $[\text{LM}_3(\text{OAc})_2(\text{solv})_n]$ 

Co3) sit in the salamo moiety, whereas the third one (Co2) is in the central cavity. Two acetato ligands as well as two phenoxo donors (O5 and O6) bridge Co1–Co2 or Co2–Co3. The two metal atoms in the N_2O_2 sites (Co1 and Co3) have a trigonal-bipyramidal geometry, whose axial positions are occupied by the N1–O5 and N4–O6 donors, respectively. On the other hand, Co2 in the central O_6 site has an octahedral geometry with six oxygen-donor atoms including two μ_2 -acetato ligands and two ethanol molecules. There are hydrogen bonds between the ethanol molecules and phenoxo oxygen atoms [O15–O9 2.729(7) Å and O16–O1 2.719(7) Å].

There are common features in the crystal structures of the trinuclear complexes $[\text{LM}_3(\text{OAc})_2(\text{solv})_n]$ ($\text{M} = \text{Mn}^{\text{II}}$, solv = MeOH, $n = 2$; $\text{M} = \text{Co}^{\text{II}}$, solv = EtOH, $n = 2$; $\text{M} = \text{Zn}^{\text{II}}$, ^{15a,d} solv = EtOH or H_2O , $n = 1$). All of the complexes have the third metal ion in the central O_6 cavity, and the three metal ions are bridged by the μ_2 -phenoxo ligand and at least one μ_2 -acetato ligand. It was known that the phenoxo oxygen of metal complexes of the salen-type N_2O_2 ligands can further coordinate to another metal ion much stronger than the phenol of uncomplexed ligands. This is mainly due to the anionic feature of the deprotonated phenol group, which can readily bridge two metal ions in a μ_2 fashion. Furthermore, the bridging μ_2 -acetato ligands contribute to the stabilization of the trinuclear structure. We have reported that the O_6 site of the ligand L^{4-} is suitable for the inclusion of rare-earth and alkaline-earth metal ions because of the effective coordination of all six oxygen donors (four μ_2 -phenoxo and two methoxy groups) arranged in a cyclic fashion. In the homotrimeric system, however, the simultaneous coordination of the six oxygen donors to the central metal ion is not essential for the formation of $[\text{LM}_3]^{2+}$.^{15a,d} The two terminal salicylidene moieties of $[\text{LM}_3]^{2+}$ are dangling because they do not simultaneously coordinate to the central metal ion.

Because of this structural feature, the ligand moiety of complexes $[\text{LM}_3]^{2+}$ has various structures depending on the metal used. The dihedral angles α and α' between the benzene rings (defined as shown in Scheme 4) are summarized in Table 3. The terminal benzene ring of the zinc(II) complexes $[\text{LZn}_3(\text{OAc})_2(\text{solv})]$ (solv = H_2O and EtOH)^{15a,d} is bent to the same side and the angles α and α' range from

Table 3. Dihedral Angles α and α' of Trinuclear Transition-Metal Complexes $[\text{LM}_3(\text{OAc})_2(\text{solv})_n]$

complex	α (deg) ^a	α' (deg) ^a
$[\text{LMn}_3(\text{OAc})_2(\text{MeOH})_2]$	78.16(9)	33.66(11)
$[\text{LCo}_3(\text{OAc})_2(\text{EtOH})_2]$	93.0(2)	−92.0(2)
$[\text{LZn}_3(\text{OAc})_2(\text{H}_2\text{O})]$ ^{15d}	66.0(2)	105.2(2)
$[\text{LZn}_3(\text{OAc})_2(\text{EtOH})]$ ^{15a}	69.47(13)	88.19(12)

^a Dihedral angles α and α' are defined as shown in Scheme 4.

66 to 105°. In the case of the manganese(II) complex, one of the angles is much smaller than the other [78.16(9) and 33.66(11)°]. The pentagonal-bipyramidal geometry of Mn2, in which four of the five equatorial positions are occupied by oxygen atoms (O1, O2, O5, and O6) of L^{4-} , probably increases the planarity around the Mn1–salamo moieties. On the other hand, only O5 and O6 coordinate to the central metal in the case of the cobalt(II) complex. Interestingly, the two terminals of the ligand L^{4-} in $[\text{LCo}_3(\text{OAc})_2(\text{EtOH})_2]$ are directed to opposite sides with almost the same angles ($\alpha = 93.0^\circ$ and $\alpha' = -92.0^\circ$). Accordingly, the cobalt(II) complex has an S-shaped structure in which both ends of the ligand L^{4-} are separated from each other.

As a result, the structure of the trinuclear complex $[\text{LM}_3(\text{OAc})_2(\text{solv})_n]$ depends on the metal. The orientation of both terminals may be influenced by the slight difference in the geometry of each metal because the phenoxo groups of at least one terminal salicylaldehyde moiety are not bound to the central metal. In addition, the coordination of the acetato ligands and solvent molecules as well as hydrogen bonds between them may affect the structure.

Synthesis and Structure of d-Block Heterometal Complexes. As described above, the homotrimeric complexes can be efficiently obtained by the cooperative complexation between the tetraoxime ligand H_4L and d-block transition-metal ions (Mn^{II} , Co^{II} , Ni^{II} , and Zn^{II}) in spite of the two completely different coordination environments provided by the N_2O_2 chelates and an O_6 cavity. We have reported that the heterotrimeric complex $[\text{LZn}_2\text{G}]^{n+}$ ($\text{G} =$ alkaline earth and rare earth) can be obtained by the selective metal exchange that is probably driven by the larger electric charge and suitable ionic radius of G^{n+} .^{15d} The different nature of the two kinds of coordination sites effectively discriminates the different d-block transition metals, even though they have the same electric charges and similar ionic radii. In fact, the site-selective synthesis of heteronuclear complexes $[\text{LM}_2\text{M}']^{2+}$, where M and M' are different d-block transition metals, can also be achieved using the bis(salamo) ligand H_4L (Scheme 5).

Table 4 shows the predominant species observed in the ESI mass spectra of the ligand H_4L in the presence of two of the five divalent d-block transition metals (Mn^{II} , Co^{II} , Ni^{II} , Cu^{II} , and Zn^{II} ; 3 equiv each). For $\text{Cu}^{\text{II}}-\text{Co}^{\text{II}}$, $\text{Co}^{\text{II}}-\text{Ni}^{\text{II}}$, and $\text{Ni}^{\text{II}}-\text{Zn}^{\text{II}}$, a mixture of trinuclear complexes was formed. However, it is noteworthy that a single heterotrimeric complex $[\text{LM}_2\text{Mn}]^{2+}$ was selectively formed in a solution containing Mn^{II} and M^{II} (Cu^{II} , Co^{II} , Ni^{II} , and Zn^{II}). The reverse heterotrimeric complexes $[\text{LMn}_2\text{M}]^{2+}$ or homotrimeric complexes $[\text{LM}_3]^{2+}$ were not detected in the mass spectra. The almost exclusive formation of $[\text{LM}_2\text{Mn}]^{2+}$

Scheme 5. Formation of Trinuclear Complexes with Two Different d-Block Transition Metals

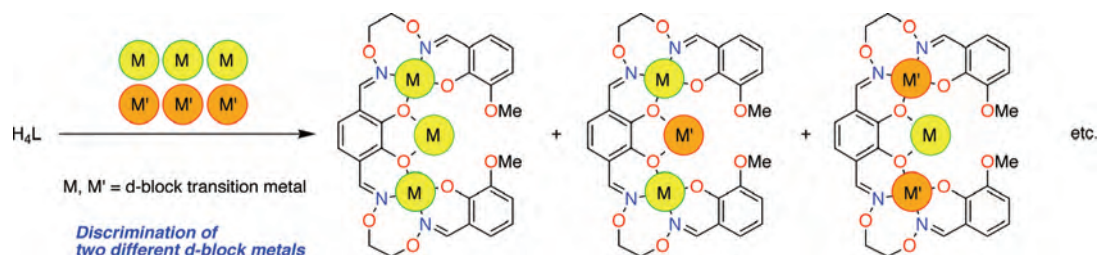


Table 4. Predominant Species Observed in ESI Mass Spectra of H_4L in the Presence of Two Kinds of d-Block Transition Metals (3 equiv for Each)

M	M'	LM_2M' species ^a	others
Cu	Co	LCu_2Co , LCO_2Cu	L_2Cu_4Co , LCu_2^b
Cu	Ni	$(LNi_2Cu)^c$	LCu_2^b
Cu	Zn	LCu_2Zn	LCu_2^b
Cu	Mn	LCu_2Mn	LCu_2^b
Co	Ni	LCO_3 , LCO_2Ni	
Co	Zn	LCO_2Zn , $(LZn_2Co)^c$	
Co	Mn	LCO_2Mn	
Ni	Zn	LZn_2Ni , LNi_2Zn	
Ni	Mn	LNi_2Mn	
Zn	Mn	LZn_2Mn	$(LZn_2)^{b,c}$

^a Observed as $[LM_2M']^{2+}$ and $[LM_2M'(OAc)]^+$. ^b Observed as $[LM_2H]^+$, $[LM_2Na]^+$, and/or $[LM_2Ca]^{2+}$. ^c Weak intensity.

Table 5. Selected Interatomic Distances (Å) of $[LZn_2Mn(OAc)_2(MeOH)_2]$ and $[LCu_2Zn(OAc)_2(H_2O)]$

$[LZn_2Mn(OAc)_2(MeOH)_2]$		$[LCu_2Zn(OAc)_2(H_2O)]$	
Zn1–N1	2.052(3)	Cu1–N1	1.962(6)
Zn1–N2	2.133(3)	Cu1–N2	2.014(7)
Zn1–O1	2.074(2)	Cu1–O1	1.949(5)
Zn1–O5	1.987(2)	Cu1–O5	1.902(5)
Zn1–O11	1.966(3)	Cu1–O11	2.252(6)
Zn2–N3	2.071(3)	Cu2–N3	1.998(7)
Zn2–N4	2.177(3)	Cu2–N4	1.972(7)
Zn2–O6	2.042(2)	Cu2–O6	1.913(5)
Zn2–O9	1.967(2)	Cu2–O9	1.969(6)
Zn2–O14	1.977(3)	Cu2–O14	2.238(5)
Mn1–O1	2.206(3)	Zn1–O1	2.135(5)
Mn1–O2	2.693(3)	Zn1–O5	2.028(5)
Mn1–O5	2.175(2)	Zn1–O6	2.220(5)
Mn1–O6	2.287(2)	Zn1–O13	1.951(6)
Mn1–O13	2.127(3)	Zn1–O15	1.964(5)
Mn1–O15	2.222(3)		
Mn1–O16	2.215(3)		

suggests that Mn^{II} prefers the central O_6 cavity to the N_2O_2 salamo moiety.

The structure of $[LZn_2Mn(OAc)_2]$ was determined by X-ray crystallography (Figure 7 and Table 5). As expected, the two zinc atoms, Zn1 and Zn2, are in the N_2O_2 sites and Mn1 is in the central O_6 cavity. The geometry of Mn1 in the central O_6 site is pentagonal bipyramidal similar to that of $[LMn_3(OAc)_2(MeOH)_2]$. The five oxygen donors provided by L^{4-} (O1, O2, O5, and O6) and acetato ligand (O13) occupy the equatorial positions of Mn1, although the O2–Mn1 bond is significantly elongated [2.693(3) Å]. In addition, two methanol molecules occupy the apical positions. The preference of Zn^{II} over Mn^{II} in the N_2O_2 sites is reasonably explained by the Irving–Williams series.³² In contrast, the central O_6 site binds Mn^{II} more strongly than Zn^{II} . In the crystal structure, only two oxygen donors of the

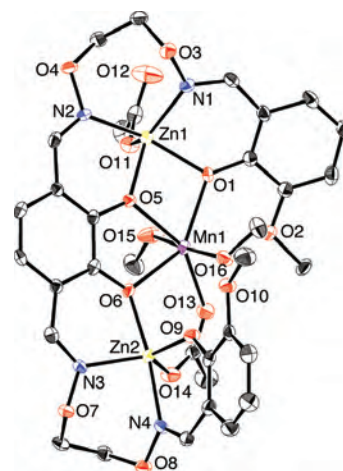


Figure 7. X-ray structure of $[LZn_2Mn(OAc)_2(MeOH)_2]$. Thermal ellipsoids are drawn at the 50% probability level.

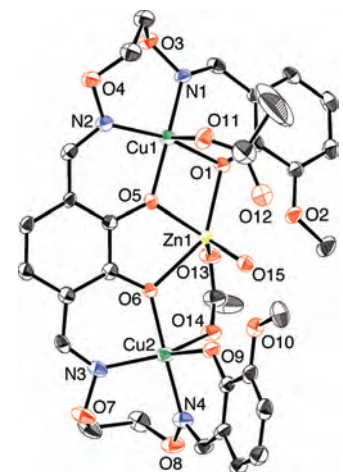


Figure 8. X-ray structure of $[LCu_2Zn(OAc)_2(H_2O)]$. Thermal ellipsoids are drawn at the 30% probability level.

O_6 site coordinate to the central Zn^{2+} of $[LZn_3]^{2+}$, while four donors interact with the central Mn^{II} of $[LZn_2Mn]^{2+}$. The $[LZn_2]$ unit binds Mn^{2+} more strongly than Zn^{2+} presumably because of the increased number of coordination bonds to the central metal.

Site selectivity was also observed when the Cu^{II} –M (M = Ni^{II} , Zn^{II} , and Mn^{II}) combinations were used as the metal source (Table 4). The predominant trinuclear complex in the ESI mass spectra was $[LCu_2M]^{2+}$. In addition, several peaks, such as $[LCu_2H]^+$ and $[LCu_2Na]^+$, were observed in the mass spectrum. These peaks strongly suggest the existence of $[LCu_2]$, which has no d-block transition metal in the O_6 site. This result shows that the affinity of the O_6 site of $[LCu_2]$ to the metals (Zn^{II} , Mn^{II} , Ni^{II} , Co^{II} , and Cu^{II}) is not so strong.

(32) Irving, H.; Williams, R. J. P. *J. Chem. Soc.* **1953**, 3192–3210.

The structure of $[\text{LCu}_2\text{Zn}]^{2+}$ was determined by X-ray crystallography (Figure 8 and Table 5). As expected, the two copper atoms (Cu1 and Cu2) are located in the salamo moieties and Zn1 is in the central O_6 cavity. Cu1 has a square-pyramidal geometry, where O11 of the monodentate acetato ligand occupies the axial position, whereas Cu2 has a trigonal-bipyramidal geometry with axial donors of O6 and N4. The geometry of Zn1 in the central O_6 site is distorted trigonal-bipyramidal in which O1 and O6 occupy the apical positions. The $[\text{LCu}_2]$ unit acts as a tridentate ligand (O1, O5, and O6) for Zn1 in the central O_6 site.

Conclusion

We have synthesized a new type of acyclic bis(N_2O_2 chelate) ligand that affords a C-shaped O_6 site by the metalation of the N_2O_2 sites. UV-vis titration clearly showed that the complexation between H_4L and a divalent d-block metal M^{II} (Mn^{II} , Co^{II} , and Ni^{II}) affords a 1:3 complex $[\text{LM}_3]^{2+}$ in a cooperative fashion. The X-ray crystallographic analysis of the manganese(II) and cobalt(II) homotrinnuclear complexes showed that each of the three metal ions occupied both the N_2O_2 and O_6 sites. The third complexation in the O_6 site is presumably due to the bridging μ_2 -acetato and μ_2 -phenoxo groups of the $[\text{M}(\text{salamo})]$ moieties. In contrast, such a 1:3 complexation with copper(II) was not favorable, probably because the acetate ion coordinates to copper(II) at a salamo N_2O_2 site more weakly than to manganese(II),

cobalt(II), nickel(II), and zinc(II). The resultant trinuclear complexes have a C- or S-shaped structure depending on the metal employed. The framework of H_4L may be utilized as a scaffold of switchable functional molecules bearing photoactive or redox-active moieties. In addition, the different nature of the N_2O_2 and O_6 sites of the ligand H_4L leads to the site-selective introduction of two different kinds of metals even if they are divalent d-block transition metals (Mn^{II} , Co^{II} , Ni^{II} , Cu^{II} , and Zn^{II}). Among them, manganese(II) selectively occupied the central O_6 site, whereas copper(II) preferred the N_2O_2 site. The resultant homo- and heterotrinnuclear complexes are attractive because we can construct next-generation functional molecules by incorporating the intrinsic properties of the metal complexes such as catalytic activity and redox properties.

Acknowledgment. We thank Dr. Kenji Yoza (Bruker AXS KK) for the X-ray data collection of H_4L . This work was supported by Grants-in-Aid for Scientific Research from the Ministry of Education, Culture, Sports, Science and Technology, Japan.

Supporting Information Available: X-ray crystallographic data in CIF format. This material is available free of charge via the Internet at <http://pubs.acs.org>.

IC702255S